

Culture of equine fibroblast-like synoviocytes on synthetic tissue scaffolds towards meniscal tissue engineering: a preliminary cell- seeding study

Introduction: Tissue Engineering is a new methodology for addressing meniscal injury or loss. Synovium may be an ideal source of cells for *in vitro* meniscal fibrocartilage formation, however, favorable *in vitro* culture conditions for synovium must be established in order to achieve this goal. The objective of this study was to determine cellularity, cell distribution, and extracellular matrix (ECM) formation of equine fibroblast-like synoviocytes (FLS) cultured on synthetic scaffolds, for potential application in synovium-based meniscal tissue engineering. Scaffolds included open-cell poly-L-lactic acid (OPLA) sponges and polyglycolic acid (PGA) scaffolds cultured in static and dynamic culture conditions, and PGA scaffolds coated in poly-L-lactic (PLLA) in dynamic culture conditions. **Materials and Methods:** Equine FLS were seeded on OPLA and PGA scaffolds, and cultured in a static environment or in a rotating bioreactor for 12 days. Equine FLS were also seeded on PGA scaffolds coated in 2% or 4% PLLA and cultured in a rotating bioreactor for 14 and 21 days. Three scaffolds from each group were fixed, sectioned and stained with Masson's Trichrome, Safranin-O, and Hematoxylin and Eosin, and cell numbers and distribution were analyzed using computer image analysis. Three PGA and OPLA scaffolds from each culture condition were also analyzed for extracellular matrix (ECM) production via dimethylmethylene blue (sulfated glycosaminoglycan) assay and hydroxyproline (collagen) assay. PLLA coated PGA scaffolds were analyzed using double stranded DNA quantification as a reflection of cellularity and confocal laser microscopy in a fluorescent cell viability assay. **Results:** The highest cellularity occurred in PGA constructs cultured in a rotating bioreactor, which also had a mean sulfated glycosaminoglycan content of 22.3 μ g per scaffold. PGA constructs cultured in static conditions had the lowest cellularity. Cells had difficulty adhering to OPLA and the PLLA coating of PGA scaffolds; cellularity was inversely proportional to the concentration of PLLA used. PLLA coating did not prevent dissolution of the PGA scaffolds. All cell scaffold types and culture conditions produced non-uniform cellular distribution. **Discussion/ Conclusion:** FLS-seeding of PGA scaffolds cultured in a rotating bioreactor resulted in the most optimal cell and matrix characteristics seen in this study. Cells grew only in the pores of the OPLA sponge, and could not adhere to the PLLA coating of PGA scaffold, due to the hydrophobic property of PLA. While PGA culture in a bioreactor produced measurable GAG, no culture technique produced visible collagen. For this reason, and due to the dissolution of PGA scaffolds, the culture conditions and scaffolds described here are not recommended for inducing fibrochondrogenesis in equine FLS for meniscal tissue engineering.

1 **Culture of equine fibroblast-like synoviocytes on synthetic tissue scaffolds towards meniscal**
2 **tissue engineering: a preliminary cell- seeding study**

- 3 1) Jennifer J. Warnock, Comparative Orthopaedic Laboratory, University of Missouri,
4 Columbia, MO; Dr. Warnock's current address is College of Veterinary Medicine, Oregon
5 State University, Corvallis OR
6 2) Derek B. Fox, Comparative Orthopaedic Laboratory, University of Missouri, Columbia,
7 MO;
8 3) Aaron M. Stoker, Comparative Orthopaedic Laboratory, University of Missouri,
9 Columbia, MO
10 4) Mark Beatty, VA Nebraska-Western Iowa Health Care System and University of Nebraska
11 Medical Center College of Dentistry, Lincoln, NE
12 5) Mary Cockrell, Comparative Orthopaedic Laboratory, University of Missouri, Columbia,
13 MO
14 6) John C. Janicek, Comparative Orthopaedic Laboratory, University of Missouri, Columbia,
15 MO
16 7) James L. Cook, Comparative Orthopaedic Laboratory, University of Missouri, Columbia,
17 MO

18 This study was funded by the Comparative Orthopaedic Laboratory, University of Missouri,
19 Columbia, MO 65211

20
21 **CORRESPONDING AUTHOR:**

22 Jennifer J. Warnock,
23 Dr. Warnock's current address is:
24 Magruder Hall, College of Veterinary Medicine
25 Oregon State University, Corvallis OR 97331
26 541-737-4812
27 jennifer.warnock@oregonstate.edu

28 **Introduction:**

29 The knee menisci are semilunar-shaped fibrocartilages with extracellular matrix (ECM)
30 composed primarily of types I and II collagen, glycosaminoglycans (GAGs), and water (Fithian
31 et al. 1990). It is now well established that intact menisci are crucial for the maintenance of
32 normal joint function, however these critical structures are frequently injured in humans and
33 animals. Meniscal tears are the most common knee injury in people, and arthroscopic
34 meniscectomy represents the most common human orthopedic surgery performed annually
35 (Burks et al. 1997). Meniscal injuries are also a significant cause of lameness and decreased
36 performance in horses (Peroni & Stick 2002; Walmsley 1995; Walmsley et al. 2003); equines
37 affected by naturally occurring meniscal tears may also be a viable model for the study of human
38 meniscal injury.

39 As the axial, avascular portion of the meniscus has a limited ability to heal spontaneously,
40 (Arnoczky & Warren 1983; Kobayashi et al. 2004), the majority of meniscal injuries are treated
41 with partial meniscectomy. However, this also results in eventual articular cartilage damage of the
42 tibia and femoral condyles, and progression of debilitating osteoarthritis (Arnoczky & Warren
43 1983; Cox et al. 1975). Thus tissue engineering new meniscal fibrocartilage is being investigated
44 as a treatment for avascular meniscal injuries.

45 Synovium may be an ideal cell source for meniscal tissue engineering. Synovium plays an
46 important role in attempted vascular zone healing and regeneration (Cisa et al. 1995; Kobuna et
47 al. 1995; Ochi et al. 1996; Shirakura et al. 1997). Synovium has the ability to form
48 fibrocartilaginous-like tissue *in vivo* in response to meniscectomy (Cox et al. 1975). In addition,
49 synoviocytes have been reported to be an important element in cellular repopulation of meniscal
50 allografts (Arnoczky & Warren 1983; Rodeo et al. 2000). Synovial tissue progenitor cells, grossly
51 indistinguishable in culture from type B or fibroblast-like synoviocytes (FLS), can undergo
52 chondrogenesis *in vitro* (De Bari et al. 2001; Nishimura et al. 1999). Taken together, these data

53 indicate that synovium may be able to serve as a source for functional fibrocartilage in
54 engineering meniscal tissue, provided the chondrogenic potential of synoviocytes can be
55 optimized.

56 Tissue engineering scaffolds must provide substrate and stability for cellular retention,
57 intercellular communication, and cellular growth to allow seeded cells to proliferate extracellular
58 matrix (ECM). As the scaffolds naturally degrade, the cellular ECM must be able to take on the
59 biomechanical function and form previously designated by the scaffolds to maintain construct
60 integrity. Thus a scaffold must be hydrophilic enough to allow cell adhesion but have a long
61 enough half- life to not prematurely dissolve, which would prevent ECM proliferation and cell
62 death. PGA (poly -glycolic acid) and PLA (poly-L- lactic acid) are biodegradable,
63 biocompatible, poly-esters, that are attractive for tissue engineering because they are readily
64 available, can be easily processed into a variety of structures, and are approved by the Food and
65 Drug Administration for a number of biomedical applications (Lavik et al. 2002). PGA has been
66 successfully used as a scaffold for meniscal fibrochondrocytes *in vivo* (Kang et al. 2006) and
67 cultured *in vitro* (Aufderheide & Athanasiou 2005) to form meniscal-like tissue. Another scaffold
68 type, PLLA, (poly-L lactic acid) has been successfully used for *in vitro* tissue engineering of
69 leporine meniscal fibrochondrocytes (Esposito et al. 2013; Gunja & Athanasiou 2010),
70 chondrocytes (Sherwood et al. 2002), and human fibroblasts (Hee et al. 2006). PGA –PLLA
71 combinations have also been successfully used for *in vitro* meniscal culture (Ionescu & Mauck
72 2013). In addition, chondrocytes cultured on PGA-PLLA mixtures versus collagen sheets contain
73 more collagen type II and have stronger mechanical properties (Beatty et al. 2002) than single
74 polymer scaffolds. Further investigation of combination use of PLLA combined with PGA for *in*
75 *vitro* synoviocyte culture is warranted.

76 Cartilage and fibrocartilage engineering with biodegradable scaffolds is most successful if
77 uniform cell distribution is achieved (Davisson et al. 1999; Pazzano et al. 2000; Smith et al.

78 1995), which is optimized through the use of rotating bioreactors(Aufderheide & Athanasiou
79 2005; Kim et al. 1998; Pazzano et al. 2000). In addition, rotating bioreactors provide mechanical
80 stimulation of cultured cells. This has a positive effects on cell differentiation, cell viability,
81 extracellular matrix production, and compressive biomechanical properties, through
82 mechanotransductive effects (Davisson et al. 1999; Imler et al. 2004; Pazzano et al. 2000; Smith
83 et al. 1995). Thus scaffold culture in a rotating bioreactor may represent a useful technique for
84 synoviocyte- based engineering of functional meniscal tissue.

85 Based on this prior research, we believe that both PGA and PLLA would be viable
86 synthetic scaffolds for the *in vitro* culture of FLS for application in meniscal fibrocartilage tissue
87 engineering. Thus, the first objective of this study was to 1) determine cell distribution and ECM
88 formation of equine FLS seeded and cultured dynamically in a rotating bioreactor versus static
89 seeding and culture, on two synthetic scaffold types, PGA and open- cell PLLA (OPLA). The
90 second objective was to compare cell viability, distribution, and ECM formation of FLS cultured
91 on 2% vs 4% PLLA coated PGA scaffolds, cultured for 14 or 21 days. Our hypothesis was that
92 we would see no difference in equine FLS content, FLS distribution, and ECM formation
93 between scaffold type, biomechanical culture environment, and culture duration.

94 **Materials and Methods:**

95 ***Experiment 1:***

96 *Tissue Collection and Monolayer Cell Culture*-- Six 8.0 mm x 8.0 mm biopsies of
97 synovial intima and subintima were obtained from both stifles of an adult American Quarter
98 Horse, euthanatized according the American Veterinary Medical Association's guidelines for
99 humane euthanasia, for reasons unrelated to the study. The horse was determined to be free of
100 orthopedic disease based on pre-mortem physical examination and post mortem gross
101 examination of the joint. Tissue was placed in Dulbeccos' Modified Eagle's Media (DMEM) with
102 10% fetal bovine serum, 0.008% Hepe's buffer, 0.008% non-essential amino acids, 0.002%

103 penicillin 100I.U./mL streptomycin 100ug/mL, amphoteroicin B 25ug/mL, 0.002% L-ascorbate,
104 and 0.01% L-glutamine in preparation for monolayer culture.

105 Synovium was sectioned into 2.0mm x 2.0mm pieces using a #10 Bard Parker blade
106 under sterile conditions. The tissue fragments were combined with sterile Type 1A clostridial
107 collagenase solution (Type 1A Clostridial Collagenase, Sigma, St. Louis, MO) at a concentration
108 of 7.5mg/mL of RPMI 1640 solution. The mixture was agitated at 37°C, 5% CO₂, 95% humidity
109 for six hours. Cells were recovered through centrifugation, the supernatant decanted and the
110 cellular pellet re-suspended in 5mL of supplemented DMEM. The cell solution was transferred to
111 a 25cm² tissue culture flask containing 5mL of supplemented DMEM. The flasks were incubated
112 at 37°C, 5% CO₂, 95% humidity, with sterile medium change performed every 3 days. Synovial
113 cells were monitored for growth using an inverted microscope until observance of 95% cellular
114 confluence per tissue culture flask. At second passage cells were transferred to 75cm² tissue
115 culture flasks containing 11mL of media. At 95% confluence the cells were subcultured until the
116 4th cell passage had been reached. At 4th passage cells were removed from flasks, counted using
117 the Trypan Blue exclusion assay (Strober 2001), and transferred to scaffold culture as described
118 below.

119 *Scaffolds*—A non- woven polyglycolic acid (PGA, Tissue Scaffold, Synthecon, Houston,
120 TX) felt, 3mm thick, with 10µm diameter fibers was utilized for this study. The open-cell poly-
121 lactic acid (OPLA sponge, BD Biosciences, Bedford, MA) utilized were 5.0mmx 3.0mm, non
122 compressible, cylindrical sponges. The average OPLA sponge pore size was 100-200µm with a
123 hydration capacity of 30µl/ scaffold. PGA and OPLA scaffolds were sterilized in ethylene oxide.
124 Following sterilization, the PGA felt was cut using a sterile Baker's biopsy punch to create into
125 5.0mm x 3.0mm discs prior to cell culture to match the dimensions of the OPLA scaffolds.

126 *Dynamic Culture*-- Twelve PGA scaffolds (PGA-D group) and 12 OPLA sponges (OPLA-
127 D group) were placed in separate 110mL vessel flasks of a rotating bioreactor system (Rotating

128 Bioreactor System, Synthecon, Houston, TX (Fig. 1) containing 110mL of supplemented DMEM.
129 The scaffolds were presoaked for 24 hours in the bioreactor at 37°C, 5% CO₂, 95% humidity,
130 prior to cell introduction. Fourth passage FLS were removed from the tissue culture flasks
131 enzymatically (Accutase Innovative Cell Technologies, San Diego, CA) and counted. Cells were
132 added to the 110mL bioreactor flasks at a concentration of 1 million cells/ scaffold via a 60cc
133 syringe, slowly injected over several minutes. For the duration of the study the bioreactor vessels
134 were rotated at 51.1 rpm to allow the scaffolds to free-float and rotate within the culture medium,
135 without contacting the inner bioreactor surfaces. Cultures were maintained at 37°C, 5% CO₂,
136 95% humidity. Fifty percent of the cell culture medium volume was changed using sterile
137 technique every 3 days. Cell counts were performed on discarded media for the first two media
138 changes.

139 *Static Culture*-- Twelve PGA scaffolds (PGA-S group) and 12 OPLA sponges (OPLA-S
140 group) were placed individually in non- treated 24 well tissue culture plates, each well containing
141 2mL of supplemented DMEM (Fig. 2). The scaffolds were presoaked for 24 hours at 37°C, 5%
142 CO₂, 95% humidity, prior to cell introduction. Then FLS were transferred from monolayer
143 culture as described above, and slowly over 3 minutes, pipetted on top of the scaffolds in
144 solution, at 1 million cells per scaffold in each well. The plates were maintained at 37°C, 5%
145 CO₂, 95% humidity, with 50% cell culture medium changed every 3 days. Cell counts were
146 performed on discarded media for the first 2 media changes.

147 *Histologic Analysis*-- All scaffolds were harvested on the 12th day of culture. Six scaffolds
148 from each group (PGA-S, PGA-D, OPLA-S, OPLA-D) were fixed in 10% buffered formalin,
149 embedded in paraffin, sectioned, and stained with Masson's Trichrome, Safranin -O, and
150 Hematoxylin and Eosin. Histologic specimens were examined at 10x magnification (Zeiss
151 Microscope, Carl Zeiss, Thornwood, NY). Images of each section, (three from the scaffold
152 periphery and three from the scaffold center) at 2 o'clock, 6o'clock and 10o'clock positions (Fig.

153 3) were digitally captured by a digital camera (Olympus DP-70 Olympus, Melville, NY) and
154 saved as tagged- image file format images. Digital image analysis was performed as previously
155 validated (Amin et al. 2000; Benzinou et al. 2005; Girman et al. 2003; Goedkoop et al. 2005)
156 whereby cellular density was assessed using a thresholding algorithm (Loukas et al. 2003) using
157 computer image analysis (Fovea 3.0, Reindeer Graphics, Asheville, NC). This algorithm allows
158 quantification of cellular nuclei based on their histogram values. All cell counts were
159 additionally validated by hand counts. Safranin-O staining, indicating presence of GAG, and
160 Masson's Trichrome staining, indicating presence of collagen, were subjectively evaluated and
161 recorded.

162 *Biochemical ECM Analysis*-- Three cultured scaffolds from each group were analyzed for
163 glycosaminoglycan (GAG) and collagen production. Wet weight of each scaffold was obtained.
164 GAG content of the scaffold was performed using the Dimethylmethylene Blue Sulfated
165 Glycosaminoglycan assay (Farndale et al. 1986). Collagen content of the cultured scaffolds was
166 assessed using the hydroxyproline assay, as described by Reddy et al.(Reddy & Enwemeka
167 1996).

168 *Statistical Methods*—Data were tested for normality using a Shapiro-Wilk test.
169 Data were then analyzed using a one way analysis of variance followed by a Tukey's test, to
170 compare the effect of scaffold type and seeding technique on cell counts and ECM quantity. To
171 determine significance between periphery and central cell counts within each scaffold, a paired,
172 2-tailed student's t-test was performed. For all tests significance was set at $P < 0.05$. All
173 statistical analyses were performed using a statistical software program, (GraphPad Prism
174 Version 6, San Diego, CA).

175 .

176 ***Experiment 2:***

177 *Scaffolds*-- Poly-L –Lactic acid (PLLA) was dissolved in methylene chloride as a 2% or
178 4% solution. The 2% and 4% PLLA solution each was applied to a 3.0 mm thick sheet of the
179 same, above- described, non- woven PGA felt, using an eye-dropper. Following PLLA treatment,
180 the treated felt was placed in a vacuum dessicator overnight and then sterilized in ethylene oxide.
181 Following sterilization, the 2% and 4% PLLA modified PGA felts were cut into fourteen 5mmx
182 7mmx 3mm square scaffolds using sterile scissors and a #10 bard parker blade (Fig 4).

183 *Tissue Collection and Monolayer Cell Culture* -- Synovial intima/ subintima was
184 harvested from the stifles of two mixed breed, adult horses euthanatized according the American
185 Veterinary Medical Association’s guidelines for humane euthanasia, for reasons unrelated to the
186 study. These horses were also determined to be free of orthopedic disease based on pre-mortem
187 physical examination and post mortem gross examination of the joint. The tissue was
188 transported, minced and digested as described above. Cells were recovered through
189 centrifugation, the supernatant decanted and the cellular pellet re-suspended in 5mL of
190 supplemented DMEM. The cell solution was transferred to a 25mL tissue culture flask containing
191 5mL of supplemented DMEM. Cells were grown in monolayer culture, under the conditions
192 described above, until the 4th cell passage had been reached.

193 *Dynamic Culture*-- Fourteen 2% PPLA coated PGA scaffolds and fourteen 4% PPLA
194 coated PGA scaffolds were placed in separate 110mL vessel flasks of the rotating bioreactor
195 system containing 110mL of supplemented DMEM. The scaffolds were presoaked for 24 hours in
196 the bioreactor at 37°C, 5% CO₂, 95% humidity, prior to cell introduction. After this time it was
197 noted that the scaffolds were floating at the apex of the flasks. Using sterile surgical technique,
198 scaffolds were sterily removed from the flasks, pierced centrally, and strung on loops of 3-0
199 nylon surgical suture with knots placed adjacent to the scaffolds to prevent bunching on the line.
200 Seven scaffolds were placed per suture. The strings of scaffolds were then placed back in to the

201 bioreactors and presoaked for another 12 hours, at which time complete hydration and
202 submersion were achieved (Fig. 5).

203 Scaffolds were then dynamically seeded. Synovial membrane cells were removed from
204 the tissue culture flasks using as described above and counted using the Trypan Blue exclusion
205 assay (Strober 2001). Cells were added to the bioreactor flasks at a concentration of 475,000 cells
206 per mL.

207 For the duration of culture, the bioreactor was maintained at 37°C, 5% CO₂, 95%
208 humidity at 51.1 rpm. Fifty percent of the cell culture medium volume was changed using sterile
209 technique every 3 days. Seven scaffolds were harvested on day 10 of culture, and 7 scaffolds
210 were harvested on day 21 of culture.

211 *Determination of Cell Viability*-- Cell viability was determined with the use of ethidium
212 homodimer-1 (4ul/ml PBS) and Calcein AM (Acetoxymethylester) (0.4ul/ml PBS) fluorescent
213 stains (Invitrogen, Carlsbad CA) and the use of Confocal Laser Microscopy. The Confocal Laser
214 Microscope consists of the BioRad Radiance 2000 confocal system coupled to an inverted
215 microscope (Olympus IX70 Olympus, Melville, NY) equipped with Krypton-Argon and red
216 diode laser. Approximately 1.0 mm sections were made from the halved scaffold using a rotary
217 paper cutter. A section from each scaffold's cut center and a section from each scaffold's
218 periphery was examined. Sections were incubated with the staining agents for 30 minutes at room
219 temperature, placed on a glass microscope slide, moistened with several drops of PBS, and
220 stained using the fluorescent double labeling technique. The sections were examined under 10x
221 magnification. Images were taken of each specimen as described above, (three from the section
222 periphery and three from the section center) at the 2 o'clock, 6 o'clock and 10 o'clock positions.
223 Images were digitally captured as described above. Live and dead cell counts were determined by
224 hand counts.

225 *DNA Quantification* -- One half of each construct was lyophilized and a dry weight
226 obtained. Samples were incubated in 1.0ml Papain Solution (2mM Dithiothreitol and 300ug/ml
227 Papain) at 60°C in a water bath for 12 hours. A double stranded DNA quantification assay
228 (Quant-iT PicoGreen™ Invitrogen, Carlsbad, CA) was performed. Double stranded DNA
229 extracted from bovine thymus was mixed with TE buffer (Invitrogen, Carlsbad, CA) to create
230 standard DNA concentrations of 1,000, 100, 10, and 1 ng/mL. The standards and 100uL of each
231 papain digested sample (used in the above GAG and hydroxyproline assays) were added to a
232 black 96 well plate. 100uL of 2ug/mL of Pico Green reagent was added to each well and the
233 plate was incubated for 5 minutes. Sample fluorescence was read at 485nm excitation/ 528nm
234 emission by a spectrophotometric plate reader (Synergy HT – KC-4, BioTek, Winooski, VT).
235 Absorbances were converted to ng/mL concentrations and total double stranded DNA yield in ng
236 using FT4 software (BioTek, Winooski, VT).

237 *Statistical Methods*— Data were tested for normality using a Shapiro-Wilk test. Scaffold
238 weights were compared using a 2-tailed paired t-test. Scaffold dsDNA content was analyzed
239 using a repeated- measures analysis of variance with a Geisser-Greenhouse correction.
240 Significance was set at $p < 0.05$. All statistical analyses were performed using a statistical
241 software program, (GraphPad Prism Version 6, San Diego, CA).

242 **Results**

243 *Experiment 1:*

244 As determined by the Trypan Blue exclusion assay, viability of cells at the time of transfer
245 from monolayer culture to static or dynamic seeding was 98.6%. No live cells were detected in
246 any of the media changes for either static or dynamically cultured scaffolds, indicating that viable
247 cells rapidly adhered to the scaffolds.

248 At the time of harvest upon gross examination, the fibers of the PGA scaffolds and the sponge
249 surface of the OPLA scaffolds were still visible. PGA scaffolds subjectively appeared more
250 translucent.

251 Despite equal cell seeding concentrations, the effect of dynamic bioreactor culture on cell
252 content of PGA scaffolds (PGA-D versus PGA-S) was to increase scaffold cellularity ($P<0.001$).
253 This was also found in OPLA-D versus OPLA-S scaffolds ($P=0.028$). The effect of scaffold type
254 also significantly increased scaffold cellularity of PGA-D versus OPLA-D ($P=0.017$), while
255 OPLA-S had great cellularity than PGA-S ($P=0.0217$; Table 1).

256 All groups, with the exception of OPLA-S, showed increased cellular distribution to the
257 periphery of the scaffolds (Table 2). Due to the shape of the OPLA-S on histological sectioning,
258 there was overlap of central and peripheral fields of view, precluding accurately localized cell
259 counts; peripheral cell count was 307 ± 52 and central cell count was 287 ± 80 ($P<0.464$). Cells
260 grew in whorls, strands, and sheets on the PGA scaffolds, while cells grew in clumps on the
261 surface pores of the OPLA sponges (Fig. 6).

262 Staining for collagen and glycosaminoglycan using Masson's Trichrome and Safranin-O,
263 respectively, was negative for extracellular matrix production in all sections of all scaffold types
264 and culture conditions evaluated.

265 In the PGA-D group, the dimethylmethylene blue assay detected a mean of $22.29 \mu\text{g}$ of GAG
266 per scaffold, (range 19.34 - $28.13 \mu\text{g}$), with a mean % GAG scaffold content of 0.0345% (μg GAG
267 per μg scaffold wet weight). No GAG was detected in OPLA constructs or PGA-S constructs.
268 The hydroxyproline assay did not detect collagen production in any group.

269 ***Experiment 2:***

270 Post PLLA modification, mean scaffold dry weights before soaking and seeding were
271 1.01mg for 2% PLLA coating and 1.52mg for 4% PLLA coating ($P<0.001$). Scaffold dry weights

272 decreased over time. Mean lyophilized weight on day 10 for 2% PLLA coating was 0.533mg,
273 which decreased to 0.257mg on day 21 ($P=0.02$). Mean lyophilized weight on day 10 for 4%
274 PLLA coating was 0.481mg, which decreased to 0.381mg on day 21 ($P=0.043$).

275 Scaffold cellularity as measured by dsDNA content increased over time: for the 2%
276 group, day 10 cellularity was 102.6 ng dsDNA/mg dry weight, and on day 21 it was 281.79
277 ($P=0.021$). On day 10 for the 4% group, dsDNA content was 111.01 ng dsDNA/mg dry weight
278 and on day 21 it was 140.2ng dsDNA/mg dry weight ($P= 0.032$; Fig. 7).

279 PLLA coating also affected scaffold dsDNA content. Scaffolds with the 2% PLLA coating
280 had greater dsDNA content than the 4% PLLA coating on day 21 ($P=0.003$), but not on day 10
281 ($P=0.602$; Fig 7).

282 As visible under confocal microscopy, cells only adhered to the surface of exposed PGA
283 fibers and had poor to no penetration to the scaffold centers in all PLLA coated scaffolds. Viable
284 cell numbers were estimated only because of the marked cellular clumping; all scaffolds showed
285 mixtures of viable and non- viable cells localized in clumps on the scaffold outer margins (Figs 8-
286 11). Histologic examination of H+E stained constructs revealed minimal cellular adhesion to the
287 PLLA, in all groups at all times, with cells growing primarily on the exposed PGA scaffold, in
288 tightly packed clumps, or adhering to exposed fibers of PGA. No extracellular matrix was
289 observed in any scaffolds on histologic analysis, which also reflected the uneven cellularity (Fig
290 12).

291 **Discussion:**

292 The current study analyzed the effect of scaffold type, biomechanical stimuli, and culture
293 duration on FLS seeding and production of specific meniscal ECM constituents. We found that
294 FLS-seeded PGA constructs cultured in a rotating bioreactor had the highest cellularity, with a
295 mean sulfated glycosaminoglycan content of 22.3 μ g per scaffold. PGA constructs cultured in

296 static conditions had the lowest cellularity. For PLLA coated PGA, increasing concentration of
297 PLLA decreased scaffold cellularity, while increased culture time increased scaffold cellularity, as
298 determined by the dsDNA assay. A non-uniform cellular distribution was observed for all scaffold
299 types and culture conditions.

300 Bioreactor culture provides a number of benefits over static culture, which would account for
301 the higher cellularity of PGA-D and OPLA-D versus PGA-S and OPLA-S scaffolds. The
302 rotating wall bioreactor used in this study provided a dynamic, laminar fluid shear, which
303 perfuses scaffold cultured cells (Bilodeau & Mantovani 2006), and thereby encourages cell
304 survival and proliferation by providing efficient transport of nutrients, gases, catabolites, and
305 metabolites and maintaining physiologic media pH (Gooch et al. 2001; Vunjak-Novakovic et al.
306 1998). Mixing of culture media also promotes cell seeding by creating matched relative
307 velocities of cells and scaffolds, particularly on non-woven PGA scaffolds (Vunjak-Novakovic et
308 al. 1998). In addition, the rotating wall bioreactor limits cellular stress by reducing strong shear
309 forces and cellular impact on the walls of the bioreactor (Bilodeau & Mantovani 2006).
310 However, in our study, scaffold characteristics such as scaffold density and hydrophilicity may
311 have negated the advantages of bioreactor culture, as seen with OPLA or PLLA coated scaffolds,
312 which had fewer cells and markedly uneven cell distribution, respectively.

313 A higher cell count was found on PGA-D versus OPLA-D, indicating either better adherence
314 or cell proliferation on PGA. Non-woven PGA scaffolds favor cellular capture and retention
315 because of their polar surface properties and high surface area for cellular adhesion (Day et al.
316 2004; Moran et al. 2003). Cellularity of PGA-D was further increased by the open weave and
317 low density (45-77mg/cc) of PGA scaffolds supports cellular proliferation through superior flow-
318 through of culture media and nutrient delivery (Vunjak-Novakovic et al. 1998). This is in contrast
319 to the highly dense (871mg/cc) OPLA sponges with non-communicating pores, which could
320 inhibit nutrient and gas transfer to seeded cells (Pazzano et al. 2004; Pazzano et al. 2000; Wu et

321 al. 1999). For PLLA covered PGA scaffolds, cells were located primarily on exposed PGA fibers,
322 and scaffold cellularity was inversely proportional to the concentration of PLLA. Although PLLA
323 is widely used in tissue-engineering applications because of its slower degradation
324 characteristics, strength, and mechanical properties, its hydrophobic, inert nature can affect cell-
325 matrix interactions and decrease cellular adhesion (Moran et al. 2003). While the PLLA coating
326 of PGA scaffolds was intended to protect from premature scaffold dissolution, we observed that
327 with longer duration of culture, scaffolds appeared to be more fragile to disruption with forceps
328 manipulation, particularly on the outer edges as well as around the centrally placed suture. In
329 agreement with this observation, all scaffold dry weights dropped over time, indicating scaffold
330 dissolution. Thus PLLA did not prevent PGA hydrolysis and decreased scaffold integrity. PLLA
331 coating also provided a hydrophobic barrier to centralized cell seeding and ingrowth. Thus, for
332 the future study of scaffold seeded equine FLS, use of PLLA type scaffolds is not recommended.

333 Cell distribution across all scaffolds was uneven, in contrast to previous reports on bioreactor
334 chondrocyte culture (Mahmoudifar et al. 2005; Pazzano et al. 2004). Lower central cell density
335 in our scaffolds may have indicated poor axial cell penetration and in-growth. Alternatively,
336 higher peripheral cellularity could reflect increased peripheral cell division caused by increased
337 exposure to media nutrients, gas exchange, and mechanotransductive effects (Mahmoudifar et
338 al. 2002). Additionally the OPLA scaffolds had clumped cell distribution in the outermost pores.
339 The OPLA sponge porosity may not allow uniform cell distribution; the 100-200 μ m pores do not
340 consistently communicate with each other. While OPLA-S did not have different peripheral and
341 central cell counts, this was due to an artifact of the sponge shape and precluded distinction of
342 peripheral cells from central cells. To increase central scaffold cell content, flow-through
343 bioreactors (Bilodeau & Mantovani 2006) may have greater cell seeding efficiencies than rotary
344 bioreactors. Alternatively, cells may be seeded at the time of scaffold formation, such as during
345 hydrogel synthesis, to insure central scaffold cellularity (Narita et al. 2009).

346 The culture conditions utilized in the present study resulted in minimal to no ECM formation,
347 in contrast to other studies. The mean GAG content of the PGA-D scaffold of 0.0345% (wet
348 weight basis) was lower than the 0.6-0.8% wet weight in the normal meniscus, and thus
349 represents a sub-optimal response for engineering purposes (AufderHeide & Athanasiou 2004).
350 Synoviocytes typically produce collagen type I constitutively, (Garner & al. 2000; Levick 1996),
351 however production and deposition of hydroxyproline was not detected in this study. The most
352 likely reason for this failure of ECM formation was lack of culture with a specific
353 fibrochondrogenic media. For example, culture with recombinant transforming growth factor-
354 beta, insulin-like growth factor -1 and basic fibroblast growth factor have been shown to induce
355 *in vitro* collagen formation in human synoviocytes (Pei et al. 2008). However, treatment of
356 equine FLS with the same recombinant chondrogenic growth factors, in the same culture
357 conditions as the present study, also failed to produce measureable ECM (Fox et al. 2009).
358 Reported scaffold seeding concentrations for cartilage tissue engineering include 30,000
359 fibroblasts/mL (Day et al. 2004); 600,000 chondrocytes/mL (Stading M & R 1999); 5 million
360 chondrocytes/ mL (Griffon et al. 2005); and 10 million chondrocytes/mL (Hu et al. 2005). Our
361 seeding density of 1 million equine FLS per scaffold may have been too low, as dense cell
362 aggregates are required for meniscal developmental fibrochondrogenesis (Clark & Ogden 1983)
363 due to the embryonic community effect (Gurdon et al. 1993). In the present study the FLS were
364 exposed to the mild shear forces and hydrostatic pressurization in a rotating bioreactor (Mauck et
365 al. 2002) which may not have been the optimal type of forces required for synovial collagen I
366 formation. A combination of *in vitro* tensile and compressive forces (AufderHeide & Athanasiou
367 2004; Benjamin & Ralphs 1998) may be required to support formation GAG (Valiyaveettil et al.
368 2005) and types I and II collagen (Kambic & McDevitt 2005), the major ECM components of
369 fibrocartilage. Cell culture on scaffolds may also result in cellular stress shielding, thereby
370 resulting in suboptimal matrix formation (Huey & Athanasiou 2011). Increased culture time may

371 also be beneficial to ECM formation; other studies show time dependent ECM expression
372 (Griffon et al. 2005; Mueller et al. 1999; Sha'ban et al. 2008). One study of synovial
373 chondrogenesis on PGA scaffolds utilized a longer culture duration of 60 days, with successful
374 ECM formation (Sakimura et al. 2006). Despite better cellularity, PGA scaffolds began losing
375 integrity over the culture period, even when coated with PLLA. Unless rapid ECM formation can
376 be achieved before dissolution occurs, PGA hydrolyzes too quickly ($t_{1/2} = 16$ days) for the
377 purpose of long term meniscal fibrocartilage synthesis. Treatment with chondrogenic or
378 fibrochondrogenic media may induce production of ECM, thus making the culture systems
379 described here more feasible for meniscal tissue engineering.

380 **Conclusion:**

381 In conclusion, we reject the null hypothesis; dynamic cell seeding and culture, as well as
382 increased culture duration, increased scaffold cellularity. Scaffold type also affected cellularity;
383 for bioreactor culture, PGA had higher cell counts versus OPLA, while OPLA had higher cell
384 counts versus PGA in static culture. Cells could only grow unevenly in the pores of the OPLA
385 sponge, and cells could not adhere to the PLLA coating of PGA scaffolds. Increasing the
386 concentration of PLLA coating on a PGA scaffold decreased the cellularity of the scaffold, and
387 did not prevent scaffold dissolution. While PGA culture in a bioreactor produced measurable
388 GAG, no culture technique produced visible collagen. For this reason, and due to the dissolution
389 of PGA scaffolds, the exact culture of conditions described here are not recommended for
390 inducing equine fibrochondrogenesis towards meniscal tissue engineering. Further research is
391 recommended to enhance extracellular matrix production through additional biomechanical and
392 biological stimulation, including treatment with chondrogenic media, increased culture duration,
393 and increased cell seeding concentrations.

394 This study was funded by the Comparative Orthopedic Laboratory, University of Missouri. The
395 authors have no conflicts of interest to disclose.

- 397 Amin M, Kurosaki M, Watanabe T, Tanaka S, and Hori T. 2000. A comparative study of
398 MIB-1 staining indices of gliomas measured by NIH Image analysis program and
399 conventional manual cell counting method. *Neurologic Research* 22:495-500.
- 400 Arnoczky SP, and Warren RF. 1983. The microvasculature of the meniscus and its response
401 to injury. An experimental study in the dog. *Am J Sports Med* 11:131-141.
- 402 AufderHeide AC, and Athanasiou KA. 2004. Mechanical stimulation toward tissue
403 engineering of the knee meniscus. *Ann Biomed Eng* 32:1161-1174.
- 404 Aufderheide AC, and Athanasiou KA. 2005. Comparison of scaffolds and culture conditions
405 for tissue engineering of the knee meniscus. *Tissue Eng* 11:1095-1104.
- 406 Beatty MW, Ojha AK, Cook JL, Alberts LR, Mahanna GK, Iwasaki LR, and Nickel JC.
407 2002. Small intestinal submucosa versus salt-extracted polyglycolic acid-poly-L-
408 lactic acid: a comparison of neocartilage formed in two scaffold materials. *Tissue*
409 *Eng* 8:955-968.
- 410 Benjamin M, and Ralphs JR. 1998. Fibrocartilage in tendons and ligaments--an adaptation
411 to compressive load. *J Anat* 193 (Pt 4):481-494.
- 412 Benzinou A, Hojeij Y, and Roudot A. 2005. Digital image analysis of haematopoietic
413 clusters. *Computational Methods and Programs in Biomedicine* 77:121-127.
- 414 Bilodeau K, and Mantovani D. 2006. Bioreactors for Tissue Engineering: Focus on
415 Mechanical Constraints. A Comparative Review. *Tissue Eng* 12:2367-83.
- 416 Burks RT, Metcalf MH, and Metcalf RW. 1997. Fifteen-year follow-up of arthroscopic
417 partial meniscectomy. *Arthroscopy* 13:673-679.
- 418 Cisa J, Basora J, Madarnas P, Ghibely A, and Navarro-Quilis A. 1995. Meniscal repair by
419 synovial flap transfer. Healing of the avascular zone in rabbits. *Acta Orthop Scand*
420 66:38-40.
- 421 Clark CR, and Ogden JA. 1983. Development of the menisci of the human knee joint.
422 Morphological changes and their potential role in childhood meniscal injury. *J Bone*
423 *Joint Surg Am* 65:538-547.
- 424 Cox JS, Nye CE, Schaefer WW, and Woodstein IJ. 1975. The degenerative effects of partial
425 and total resection of the medial meniscus in dogs' knees. *Clin Orthop Relat Res*
426 109:178-183.
- 427 Davisson T, Sah R, and Ratcliffe A. 1999. Perfusion increases cell content and matrix
428 synthesis in chondrocyte three- dimensional cultures. *Tissue Eng* 8:807-816.
- 429 Day R, Boccaccini A, and Shurey A. 2004. Assessment of polyglycolic acid mesh and
430 bioactive glass for soft tissue engineering scaffolds. *Biomaterials* 25:5857-5864.

- 431 De Bari C, Dell'Accio F, Tylzanowski P, and Luyten FP. 2001. Multipotent mesenchymal
432 stem cells from adult human synovial membrane. *Arthritis Rheum* 44:1928-1942.
- 433 Esposito AR, Moda M, Cattani SM, de Santana GM, Barbieri JA, Munhoz MM, Cardoso
434 TP, Barbo ML, Russo T, D'Amora U. 2013. PLDLA/PCL-T Scaffold for Meniscus
435 Tissue Engineering. *Biores Open Access* 2:138-147.
- 436 Farndale RW, Buttle DJ, and Barrett AJ. 1986. Improved quantitation and discrimination
437 of sulphated glycosaminoglycans by use of dimethylmethylene blue. *Biochim Biophys*
438 *Acta* 883:173-177.
- 439 Fithian DC, Kelly MA, and Mow VC. 1990. Material properties and structure-function
440 relationships in the menisci. *Clin Orthop Relat Res* 252:19-31.
- 441 Fox DB, Warnock JJ, Stoker AM, Luther JK, and Cockrell M. 2009. Effects of growth
442 factors on equine synovial fibroblasts seeded on synthetic scaffolds for avascular
443 meniscal tissue engineering. *Res Vet Sci* 88:326-32.
- 444 Garner P. 2000. Molecular basis and clinical use of biochemical markers of bone, and
445 synovium in joint disease. *Arthritis and Rheumatism* 43:953.
- 446 Girman P, Kriz J, Friedmanky J, and Saudek F. 2003. Digital imaging as a possible
447 approach in evaluation of islet yield. *Cell Transplantation* 12:129-133.
- 448 Goedkoop A, Rie Md, Teunissen M, and 297:51-59 eaADR. 2005. Digital image analysis for
449 the evaluation of the inflammatory infiltrate in psoriasis. *Archives of Dermatological*
450 *Research* 297:51-59.
- 451 Gooch KJ, Kwon JH, Blunk T, Langer R, Freed LE, and Vunjak-Novakovic G. 2001.
452 Effects of mixing intensity on tissue-engineered cartilage. *Biotechnol Bioeng* 72:402-
453 407.

- 454 **Griffon D, Sedighi M, Sendemir-Urkmez A, and al. e. 2005. Evaluation of vacuum and**
455 **dynamic cell seeding of polyglycolic acid and chitosan scaffolds for cartilage**
456 **engineering. *American Journal of Veterinary Research* 66:599-605.**
- 457 **Gunja NJ, and Athanasiou KA. 2010. Additive and synergistic effects of bFGF and hypoxia**
458 **on leporine meniscus cell-seeded PLLA scaffolds. *J Tissue Eng Regen Med* 4:115-122.**
- 459 **Gurdon JB, Lemaire P, and Kato K. 1993. Community effects and related phenomena in**
460 **development. *Cell* 75:831-834.**

- 461 Hee CK, Jonikas MA, and Nicoll SB. 2006. Influence of three-dimensional scaffold on the
462 expression of osteogenic differentiation markers by human dermal fibroblasts.
463 *Biomaterials* 27:875-884.
- 464 Hu J, Athaasiou K, and al. e. 2005. Low density cultures of bovine chondrocytes: effects of
465 scaffold material and culture system. *Biomaterials* 26:2001-2012.
- 466 Huey DJ, and Athanasiou KA. 2011. Maturation growth of self-assembled, functional
467 menisci as a result of TGF-beta1 and enzymatic chondroitinase-ABC stimulation.
468 *Biomaterials* 32:2052-2058.
- 469 Imler SM, Doshi AN, and Levenston ME. 2004. Combined effects of growth factors and
470 static mechanical compression on meniscus explant biosynthesis. *Osteoarthritis*
471 *Cartilage* 12:736-744.
- 472 Ionescu LC, and Mauck RL. 2013. Porosity and cell preseeding influence electrospun
473 scaffold maturation and meniscus integration in vitro. *Tissue Eng Part A* 19:538-547.
- 474 Kambic HE, and McDevitt CA. 2005. Spatial organization of types I and II collagen in the
475 canine meniscus. *J Orthop Res* 23:142-149.
- 476 Kang SW, Son SM, Lee JS, Lee ES, Lee KY, Park SG, Park JH, and Kim BS. 2006.
477 Regeneration of whole meniscus using meniscal cells and polymer scaffolds in a
478 rabbit total meniscectomy model. *J Biomed Mater Res A* 77:659-671.
- 479 Kim B, Putnam A, Kulik J, and al. e. 1998. Optimizing seeding and culture methods to
480 engineer smooth muscle tissue on biodegradable polymer matrices. *Biotechnology*
481 *and Bioengineering* 57:46-54.
- 482 Kobayashi K, Fujimoto E, Deie M, Sumen Y, Ikuta Y, and Ochi M. 2004. Regional
483 differences in the healing potential of the meniscus-an organ culture model to
484 eliminate the influence of microvasculature and the synovium. *Knee* 11:271-278.
- 485 Kobuna Y, Shirakura K, and Niijima M. 1995. Meniscal repair using a flap of synovium. An
486 experimental study in the dog. *Am J Knee Surg* 8:52-55.
- 487 Lavik E, Teng YD, Snyder E, and Langer R. 2002. Seeding neural stem cells on scaffolds of
488 PGA, PLA, and their copolymers. *Methods Mol Biol* 198:89-97.
- 489 Levick JR, Price FM, Mason FM. 1996. *Synovial matrix—synovial fluid systems of joints.*
490 In: WD Comper (ed): Extracellular Matrix. Amsterdam: Harwood Academic
491 Publishers, 235-252.
- 492 Loukas CG, Wilson GD, Vojnovic B, and Linney A. 2003. An image analysis-based
493 approach for automated counting of cancer cell nuclei in tissue sections. *Cytometry A*
494 55:30-42.

- 495 Mahmoudifar N, Doran P, and al. e. 2005. Tissue engineering human cartilage in
496 bioreactors using single and composite cell seeded scaffolds. *Biotechnology and*
497 *Bioengineering* 91:338-355.
- 498 Mahmoudifar N, Sikavistas V, Bancroif G, and Mikko A. 2002. Formation of three
499 dimensional cell/ polymer constructs for bone tissue engineering in a spinner flask
500 and a rotating wall vessel bioreactor. *Journal of Bimedical Material Research* 62:136-
501 148.
- 502 Mauck RL, Seyhan SL, Ateshian GA, and Hung CT. 2002. Influence of seeding density and
503 dynamic deformational loading on the developing structure/function relationships of
504 chondrocyte-seeded agarose hydrogels. *Ann Biomed Eng* 30:1046-1056.
- 505 Moran J, Pazzano B, and Bonassar L. 2003. Characterization of polylactic acid –
506 polyglycolic acid composites for cartilage tissue engineering. *Tissue Eng* 9:63-70.
- 507 Mueller SM, Shortkroff S, Schneider TO, Breinan HA, Yannas IV, and Spector M. 1999.
508 Meniscus cells seeded in type I and type II collagen-GAG matrices in vitro.
509 *Biomaterials* 20:701-709.
- 510 Narita A, Takahara M, Ogino T, Fukushima S, Kimura Y, and Tabata Y. 2009. Effect of
511 gelatin hydrogel incorporating fibroblast growth factor 2 on human meniscal cells in
512 an organ culture model. *Knee* 16:285-289.
- 513 Nishimura K, Solchaga LA, Caplan AI, Yoo JU, Goldberg VM, and Johnstone B. 1999.
514 Chondroprogenitor cells of synovial tissue. *Arthritis Rheum* 42:2631-2637.
- 515 Ochi M, Mochizuki Y, Deie M, and Ikuta Y. 1996. Augmented meniscal healing with free
516 synovial autografts: an organ culture model. *Arch Orthop Trauma Surg* 115:123-126.
- 517 Pazzano, Davisson, Seidel, Pei, Gray, and al e. 2004. Long term culture of tissue engineered
518 cartilage in a perfused chamber with mechanical stimulation. *Biorheology* 41:445-
519 458.
- 520 Pazzano D, Mercier K, Moran J, and al. e. 2000. Comparison of chondrogenesis in static
521 and perfused bioreactor culture. *Biotechnology Progress* 16:893-896.
- 522 Pei M, He F, and Vunjak-Novakovic G. 2008. Synovium-derived stem cell-based
523 chondrogenesis. *Differentiation* 76:1044-1056.
- 524 Peroni JF, and Stick JA. 2002. Evaluation of a cranial arthroscopic approach to the stifle
525 joint for the treatment of femorotibial joint disease in horses: 23 cases (1998-1999). *J*
526 *Am Vet Med Assoc* 220:1046-1052.
- 527 Reddy GK, and Enwemeka CS. 1996. A simplified method for the analysis of
528 hydroxyproline in biological tissues. *Clin Biochem* 29:225-229.

- 529 Rodeo SA, Seneviratne A, Suzuki K, Felker K, Wickiewicz TL, and Warren RF. 2000.
530 Histological analysis of human meniscal allografts. A preliminary report. *J Bone*
531 *Joint Surg Am* 82-A:1071-1082.
- 532 Sakimura K, Matsumoto T, Miyamoto C, Osaki M, and Shindo H. 2006. Effects of insulin-
533 like growth factor I on transforming growth factor beta1 induced chondrogenesis of
534 synovium-derived mesenchymal stem cells cultured in a polyglycolic acid scaffold.
535 *Cells Tissues Organs* 183:55-61.
- 536 Sha'ban M, Kim SH, Idrus RB, and Khang G. 2008. Fibrin and poly(lactic-co-glycolic acid)
537 hybrid scaffold promotes early chondrogenesis of articular chondrocytes: an in vitro
538 study. *J Orthop Surg* 3:17.
- 539 Sherwood JK, Riley SL, Palazzolo R, Brown SC, Monkhouse DC, Coates M, Griffith LG,
540 Landeen LK, and Ratcliffe A. 2002. A three-dimensional osteochondral composite
541 scaffold for articular cartilage repair. *Biomaterials* 23:4739-4751.
- 542 Shirakura K, Nijima M, Kobuna Y, and Kizuki S. 1997. Free synovium promotes meniscal
543 healing. Synovium, muscle and synthetic mesh compared in dogs. *Acta Orthop Scand*
544 68:51-54.
- 545 Smith R, Dunlon B, Gupta, and al. e. 1995. Effects of fluid induced shear on articular
546 chondrocyte morphology and metabolism in vitro. *Journal of Orthopaedic Research*
547 13:824.
- 548 Stading M, and R L. 1999. Mechanical shear properties of cell-polymer cartilage constructs.
549 *Tissue Eng* 5:241-250.
- 550 Strober W. 2001. Trypan blue exclusion test of cell viability. *Curr Protoc Immunol* Appendix
551 3:Appendix 3B.
- 552 Valiyaveettil M, Mort JS, and McDevitt CA. 2005. The concentration, gene expression, and
553 spatial distribution of aggrecan in canine articular cartilage, meniscus, and anterior
554 and posterior cruciate ligaments: a new molecular distinction between hyaline
555 cartilage and fibrocartilage in the knee joint. *Connect Tissue Res* 46:83-91.
- 556 Vunjak-Novakovic G, Obradovic B, Martin I, Bursac PM, Langer R, and Freed LE. 1998.
557 Dynamic cell seeding of polymer scaffolds for cartilage tissue engineering.
558 *Biotechnol Prog* 14:193-202.
- 559 Walmsley JP. 1995. Vertical tears of the cranial horn of the meniscus and its cranial
560 ligament in the equine femorotibial joint: 7 cases and their treatment by
561 arthroscopic surgery. *Equine Vet J* 27:20-25.
- 562 Walmsley JR, Phillips TJ, and Townsend HG. 2003. Meniscal tears in horses: an evaluation
563 of clinical signs and arthroscopic treatment of 80 cases. *Equine Vet J* 35:402-406.

564 Wu F, Dunkelman N, and Peterson A. 1999. Bioreactor development for tissue engineered
 565 cartilage. *Annals of the New York Academy of Science* 875:405-411.

566 **Tables**

567 Table 1: The effect of seeding and cell culture biomechanical environment and the effect of
 568 scaffold type on scaffold cellularity.

	Cell Count (Mean number of cells per 10x objective field \pm SD)		Effect of biomechanical environment (dynamic vs static culture)
Scaffold type:	Biomechanical environment:		
	Dynamic culture	Static culture	
PGA	1128 \pm 575 cells	54 \pm 34 cells	P<0.001
OPLA	375 \pm 118 cells	301 \pm 65 cells	P= 0.028
Effect of scaffold type (PGA vs OPLA)	P=0.017	P=0.0217	

569 **Table 2:**

570 Peripheral and central cell count (Mean number of cells per 10x objective field \pm SD).

Scaffold	Peripheral cell count	Central cell count	P- value
PGA-D	1433 \pm 487	724 \pm 314	P<0.001
PGA-S	80 \pm 28	28 \pm 11	P<0.001
OPLA-D	476 \pm 90	295 \pm 55	P<0.001

571 **Figures**

572 Figure 1. Rotating wall bioreactor flask (110mL) containing media and PGA scaffolds seeded
 573 with equine fibroblast-like synoviocytes (**A**). Flasks loaded on the rotating base apparatus; flasks
 574 rotate around their longitudinal axis (**B**).

575 Figure 2. Static culture of equine fibroblast- like synoviocytes on PGA scaffolds in a 24 well
 576 tissue culture plate, with each well containing 2mL of supplemented DMEM.

577 Figure 3. Method for viewing all scaffolds to standardize cell counts and determine regional cell
 578 count differences between the scaffold center and periphery. Cells were counted at the periphery
 579 and central regions (dark dotted circles) of each scaffold (cross- hatched circle) using digital

580 image analysis; peripheral cell counts (light dotted circles) were obtained at the 2o'clock,
581 6o'clock and 19o'clock positions. Circles represent a low power (10X objective) field of view.

582 Figure 4. Scanning electron microscopy of a 2% PLLA coated PGA scaffold (**A**) and a 4% PLLA
583 coated scaffold (**B**) prior to cell seeding; bar = 100µm.

584 Figure 5. Rotating wall bioreactor flask containing 2% PLLA coated PGA scaffolds, strung on
585 suture to ensure equal submersion and positioning in the rotating flask.

586 Figure 6. Micrographs of scaffolds seeded with equine fibroblast-like synoviocytes; Hematoxylin
587 and Eosin staining, 10x objective magnification; bar = 100µm. **A**) PGA scaffold cultured in a
588 static environment; **B**) PGA scaffold cultured in a dynamic environment (rotating bioreactor); **C**)
589 OPLA scaffold cultured in a dynamic environment (rotating bioreactor); **D**) OPLA scaffold
590 cultured in a static environment. Note the intact PGA fibers (open arrow) and the cells located in
591 clumps in the pores of the OPLA scaffold (closed arrows).

592 Figure 7. Mean ±Standard Error of the Mean (SEM) of dsDNA content of PGA scaffolds coated
593 in 2% PLLA and 4% PLLA, seeded dynamically and cultured in a rotating bioreactor for 14 days
594 and 21 days. A bar and (*) indicates a significant difference between two treatment
595 groups(P<0.05).

596 Figure 8. Photomicrographs of 2% PLLA coated PGA constructs harvested on day 10, under
597 standard light (column **A**) and under laser confocal microscopy (column **B**), using the calcein
598 AM-ethidium homodimer live-dead assay. Images represent scaffold transverse cross sections
599 (row **T**) and scaffold surface coronal sections (row **C**). Green stained cells are alive, red stained
600 cells are dead. 10x objective magnification; bar = 100µm.

601 Figure 9. Photomicrographs of 2% PLLA coated PGA constructs harvested on day 21, under
602 standard light (column **A**) and under laser confocal microscopy (column **B**), using the calcein
603 AM-ethidium homodimer live-dead assay. Images represent scaffold transverse cross sections
604 (row **T**) and scaffold surface coronal sections (row **C**). Green stained cells are alive, red stained
605 cells are dead. Note the spurious red staining of scaffold PGA fibers. 10x objective
606 magnification; bar = 100µm.

607 Figure 10. Photomicrographs of 4% PLLA coated PGA constructs harvested on day 10, under
608 standard light (column **A**) and under laser confocal microscopy (column **B**), using the calcein
609 AM-ethidium homodimer live-dead assay. Images represent scaffold transverse cross sections
610 (row **T**) and scaffold surface coronal sections (row **C**). Green stained cells are alive, red stained
611 cells are dead. Note the spurious red staining of PGA fibers. 10x objective magnification; bar =
612 100µm.

613 Figure 11. Photomicrographs of 4% PLLA coated PGA constructs harvested on day 21, under
614 standard light (column **A**) and under laser confocal microscopy (column **B**), using the calcein
615 AM-ethidium homodimer live-dead assay. Images represent scaffold transverse cross sections
616 (row **T**) and scaffold surface coronal sections (row **C**). Green stained cells are alive, red stained
617 cells are dead. Note the spurious red staining of PGA fibers. 10x objective magnification; bar =
618 100µm.

619 Figure 12. Photomicrographs of 2% PLLA coated PGA scaffolds harvested on day 10 (row **1**)
620 and day 21 (row **2**), and 4% PLLA coated PGA scaffolds harvested on day 10 (row **3**) and day 21
621 (row **4**), H+E staining. Column **A** represents images of the center of the construct and column **B**
622 represents images taken of the scaffold periphery. Note that the cells have grown in dense
623 clusters; 10x objective magnification; bar = 100 μ m.

Figure 1

Rotating wall bioreactor cell culture system.

Rotating wall bioreactor flask (110mL) containing media and PGA scaffolds seeded with equine fibroblast-like synoviocytes (A). Rotating wall bioreactor cell culture system with flasks loaded on the rotating base apparatus; flasks rotate around their longitudinal axis (B).

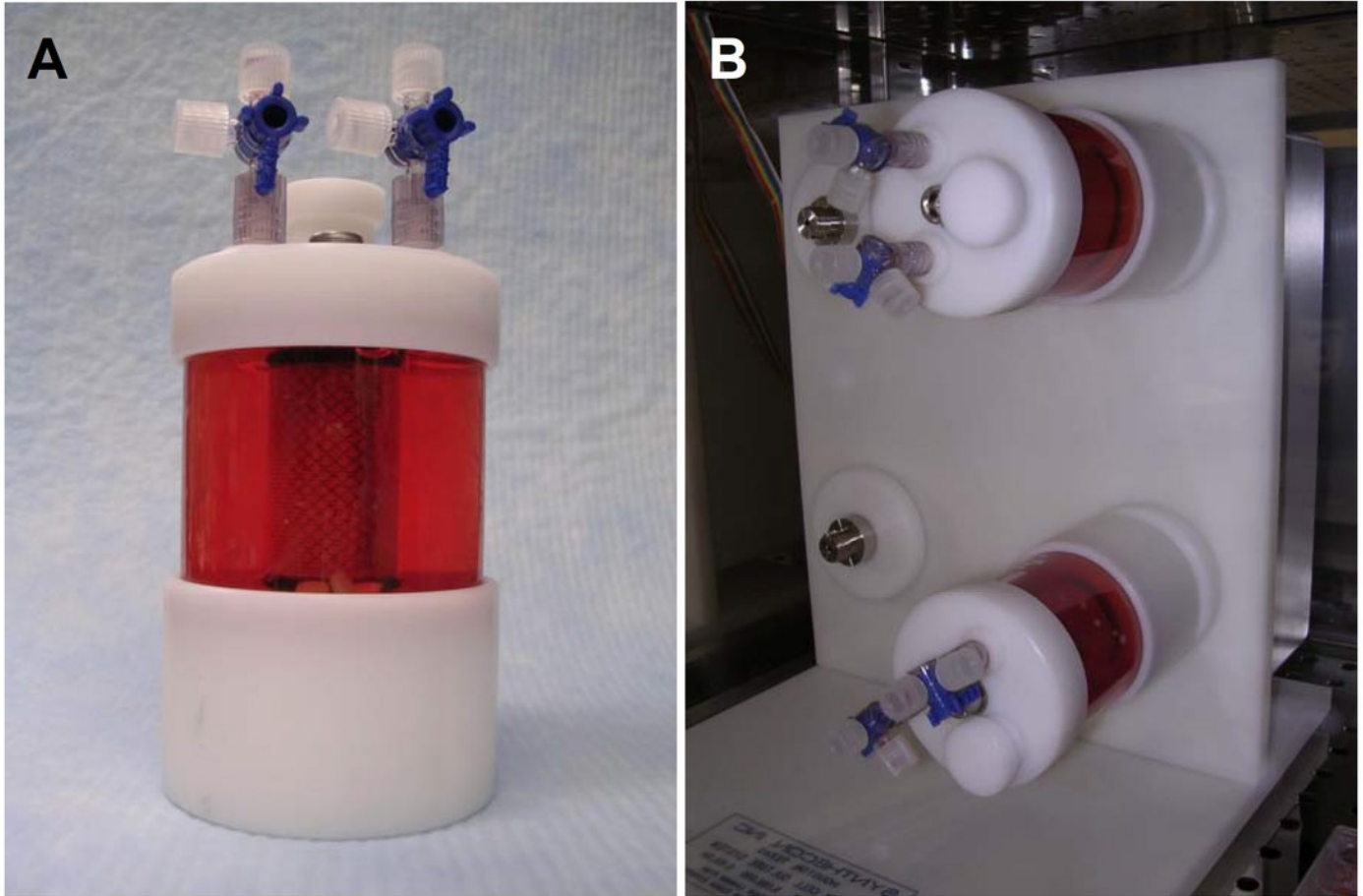


Figure 2

Static cell culture.

Static culture of equine fibroblast- like synoviocytes on PGA scaffolds in a 24 well tissue culture plate, with each well containing 2mL of supplemented DMEM.

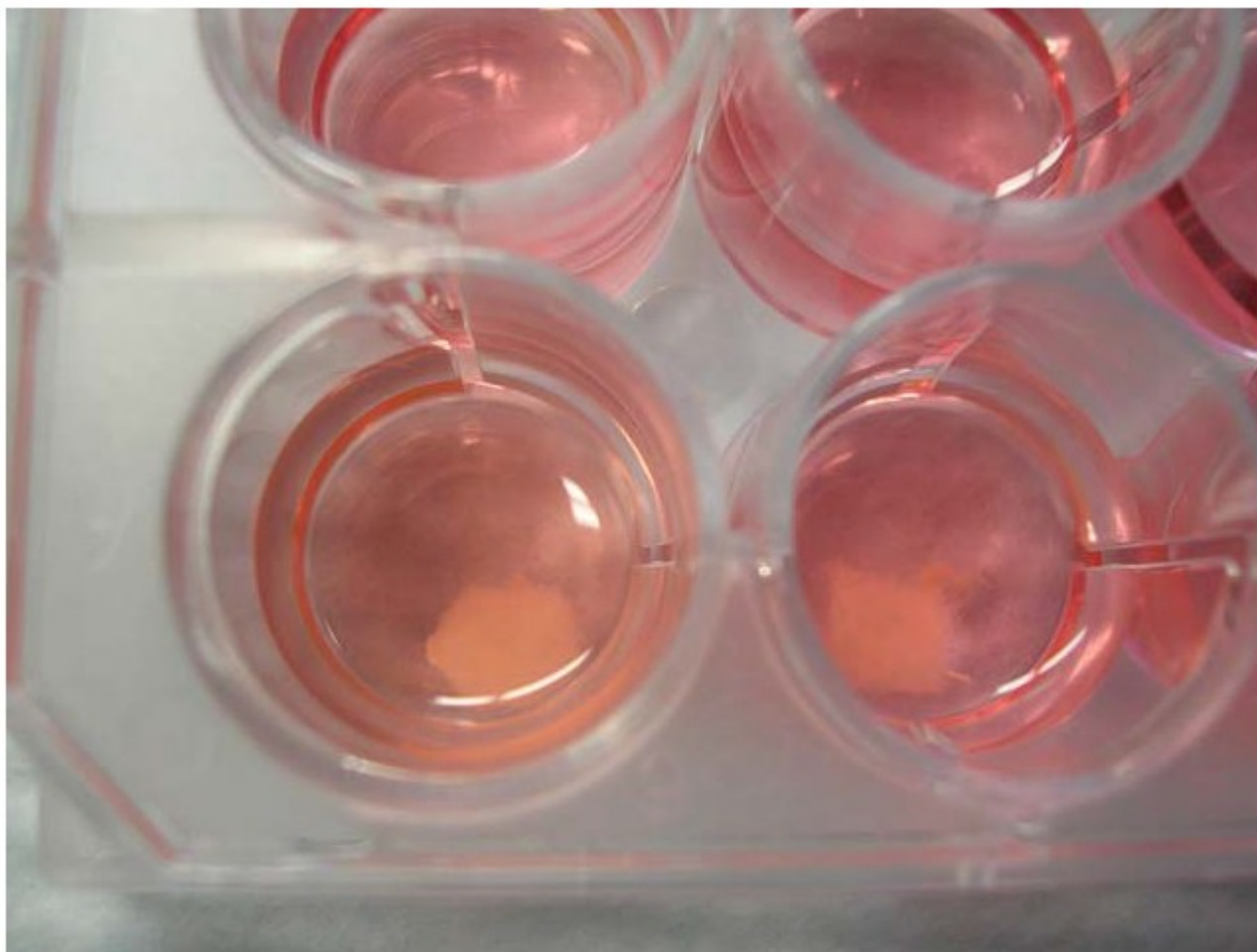


Figure 3

Method for determining peripheral and central cell counts.

Method for viewing all scaffolds to standardize cell counts and determine regional cell count differences between the scaffold center and periphery. Cells were counted at the periphery and central regions (dark dotted circles) of each scaffold (cross-hatched circle) using digital image analysis; peripheral cell counts (light dotted circles) were obtained at the 2o'clock,6o'clock and 19o'clock positions. Circles represent a 10X objective field of view.

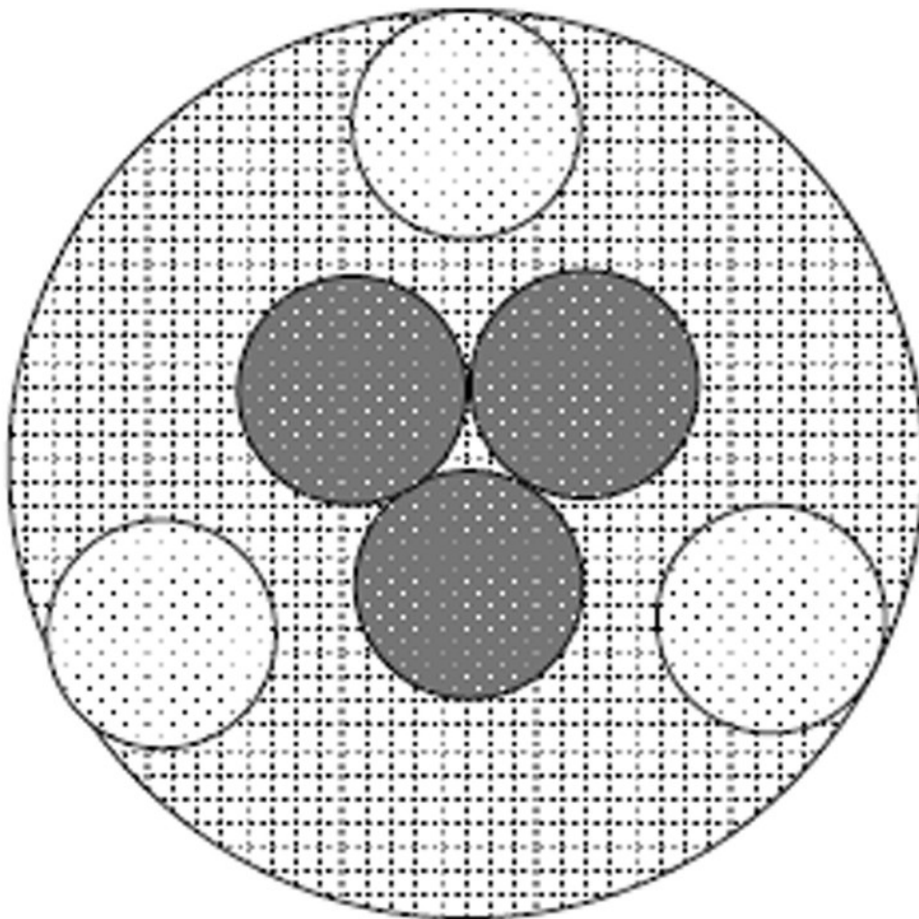


Figure 4

PLLA coated PGA scaffolds.

Scanning electron microscopy of a 2% PLLA coated PGA scaffold (**A**) and a 4% PLLA coated scaffold (**B**) prior to cell seeding; bar = 100 μ m.

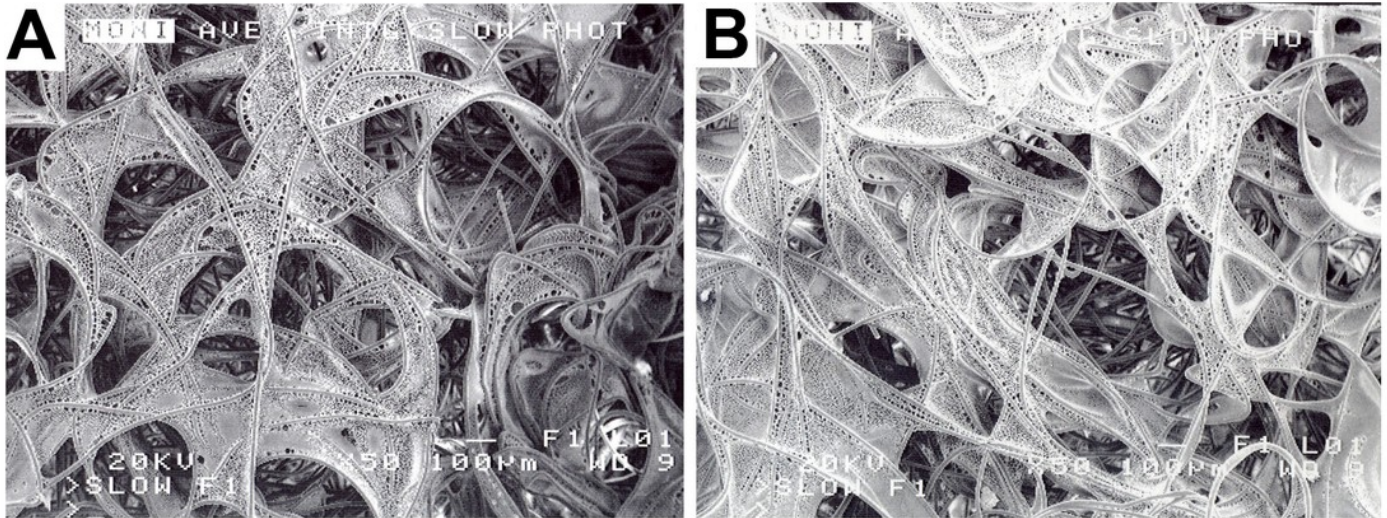


Figure 5

Method for maintaining submersion of PLLA coated PGA scaffolds.

Rotating wall bioreactor flask containing 2% PLLA coated PGA scaffolds, strung on suture to ensure equal submersion and positioning in therotating flask.

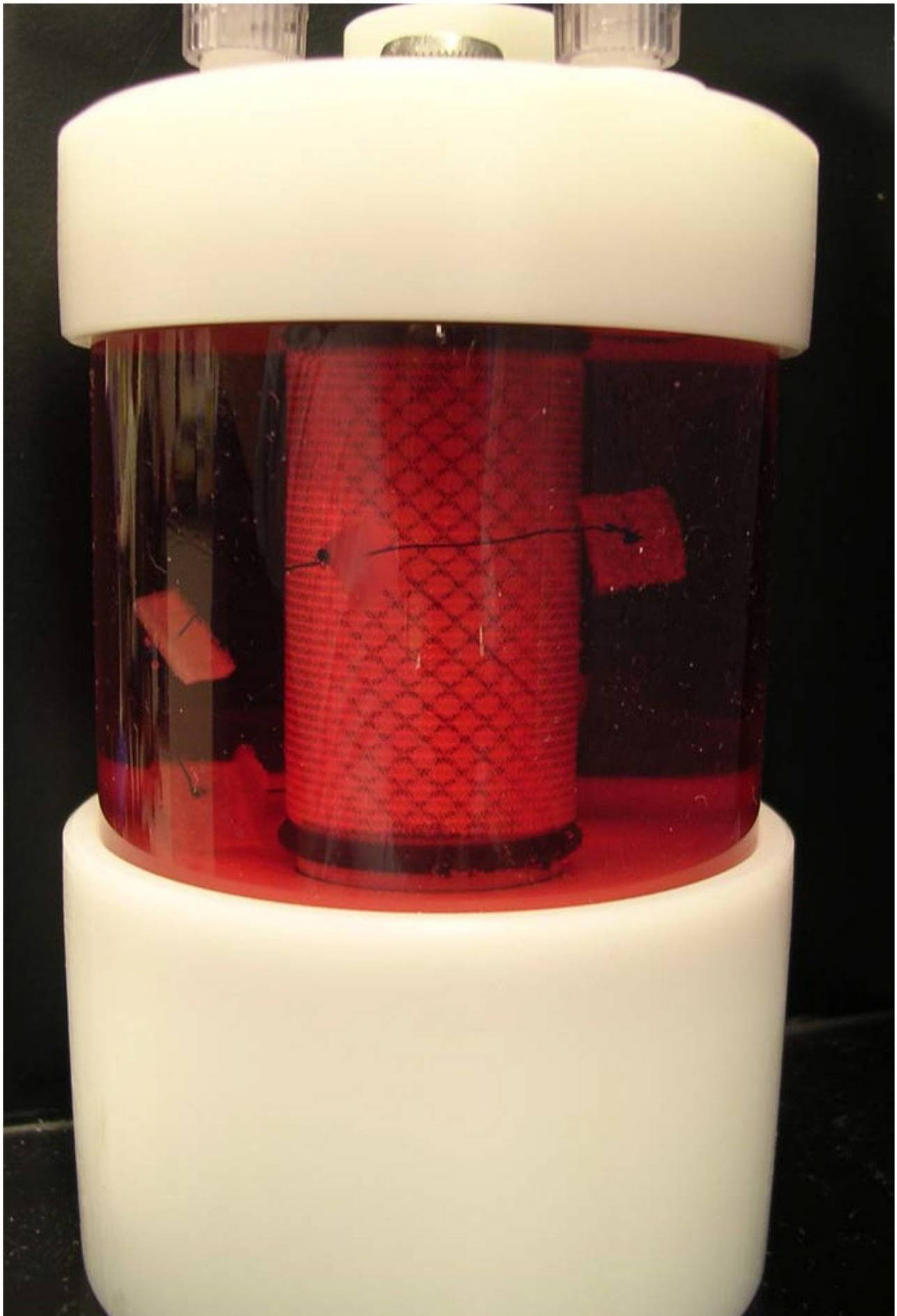


Figure 6

Cell distribution on PGA and OPLA scaffolds.

Micrographs of scaffolds seeded with equine fibroblast-like synoviocytes; Hematoxylin and Eosin staining, 10x objective magnification; bar = 100 μ m. **A**) PGA scaffold cultured in a static environment; **B**) PGA scaffold cultured in a dynamic environment (rotating bioreactor); **C**) OPLA scaffold cultured in a dynamic environment (rotating bioreactor); **D**) OPLA scaffold cultured in a static environment. Note the intact PGA fibers (open arrow) and the cells located in clumps in the pores of the OPLA scaffold (closed arrows).

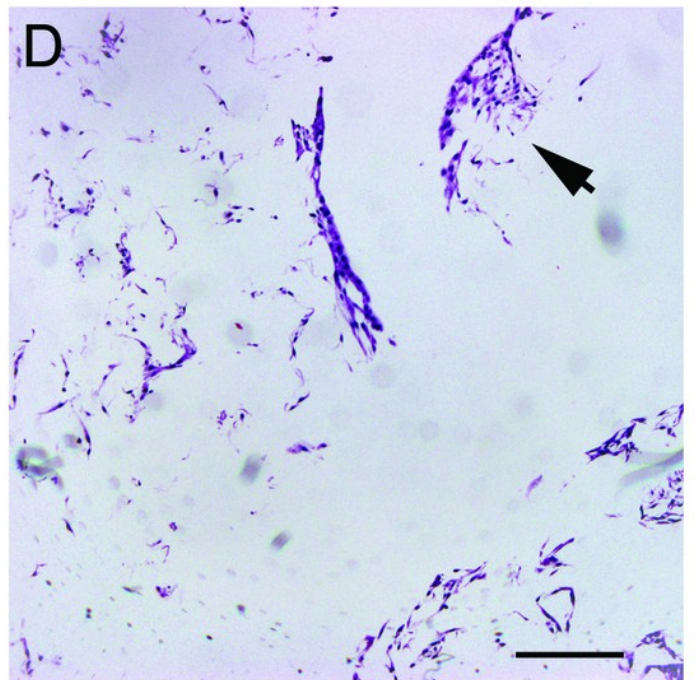
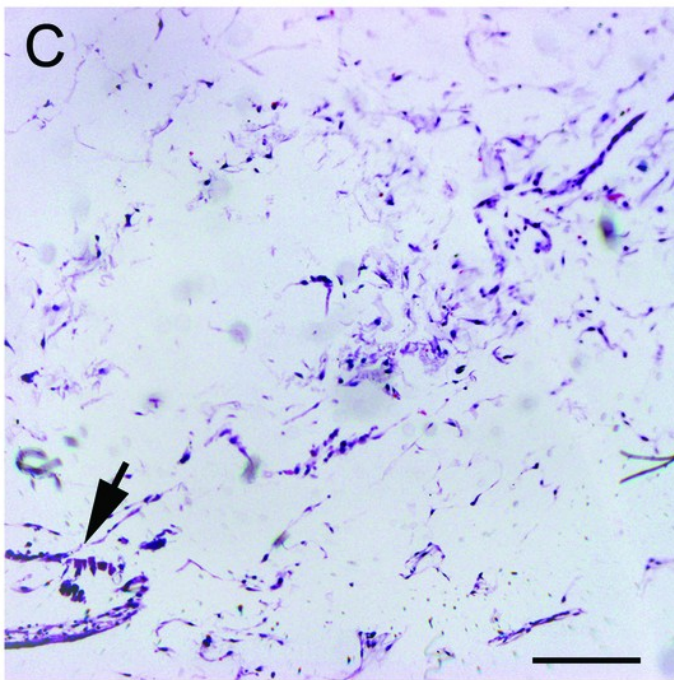
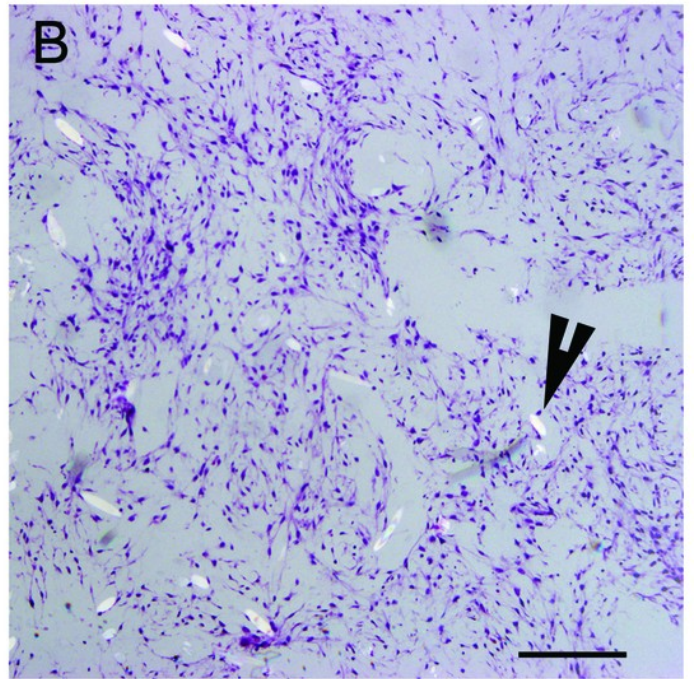
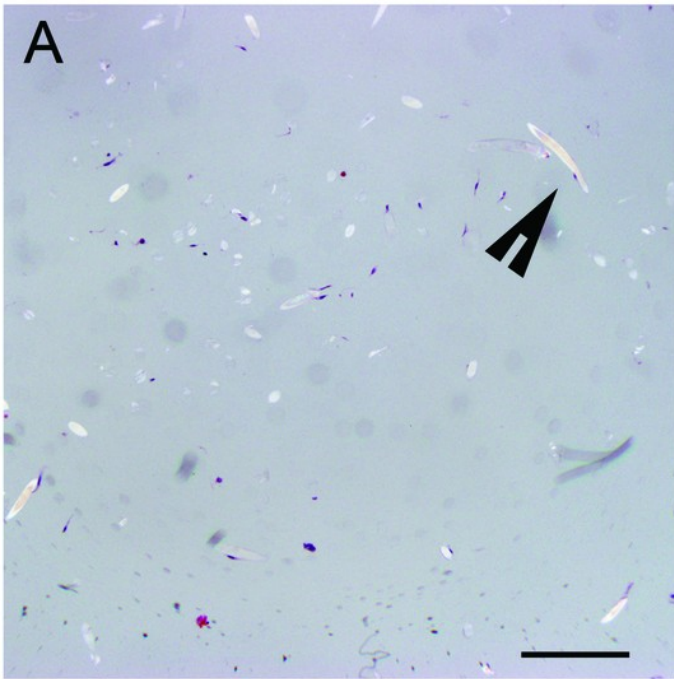


Figure 7

Double stranded DNA content of PLLA coated PGA scaffolds.

Mean \pm Standard Error of the Mean (SEM) of dsDNA content of PGA scaffolds coated in 2% PLLA or 4% PLLA, seeded dynamically and cultured in a rotating bioreactor for 14 days and 21 days. A bar and (*) indicates a significant difference between two treatment groups ($P < 0.05$).

Scaffold Cellularity as Measured by dsDNA Content

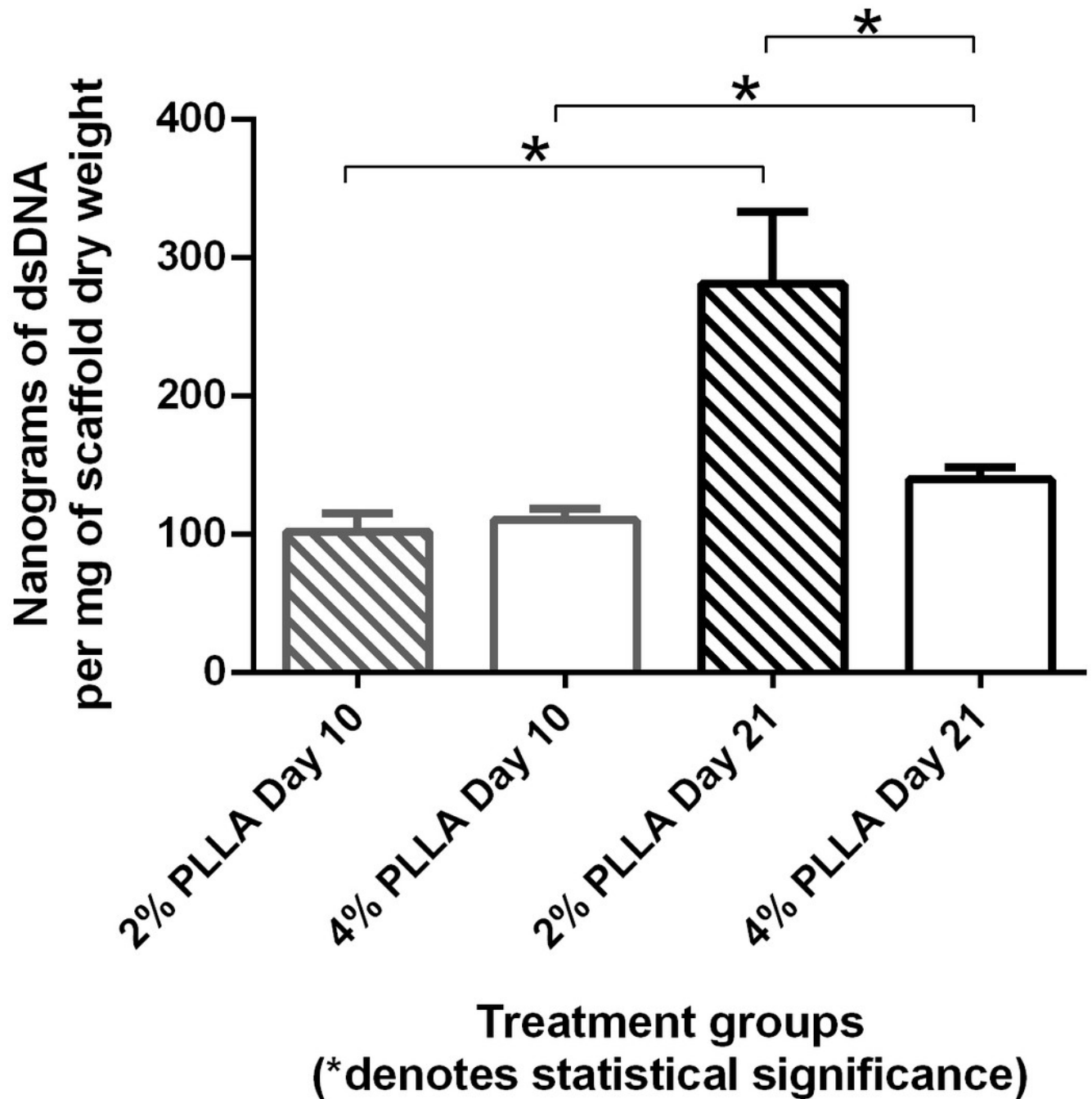


Figure 8

Synoviocytes cultured on 2% PLLA coated PGA on day 10 of dynamic culture.

Photomicrographs of 2% PLLA coated PGA constructs harvested on day 10, under standard light (column A) and under laser confocal microscopy (column B), using the calcein AM ethidium homodimer live-dead assay. Images represent scaffold transverse cross sections (row T) and scaffold surface coronal sections (row C). Green stained cells are alive, red stained cells are dead. 10x objective magnification; bar = 100 μ m.

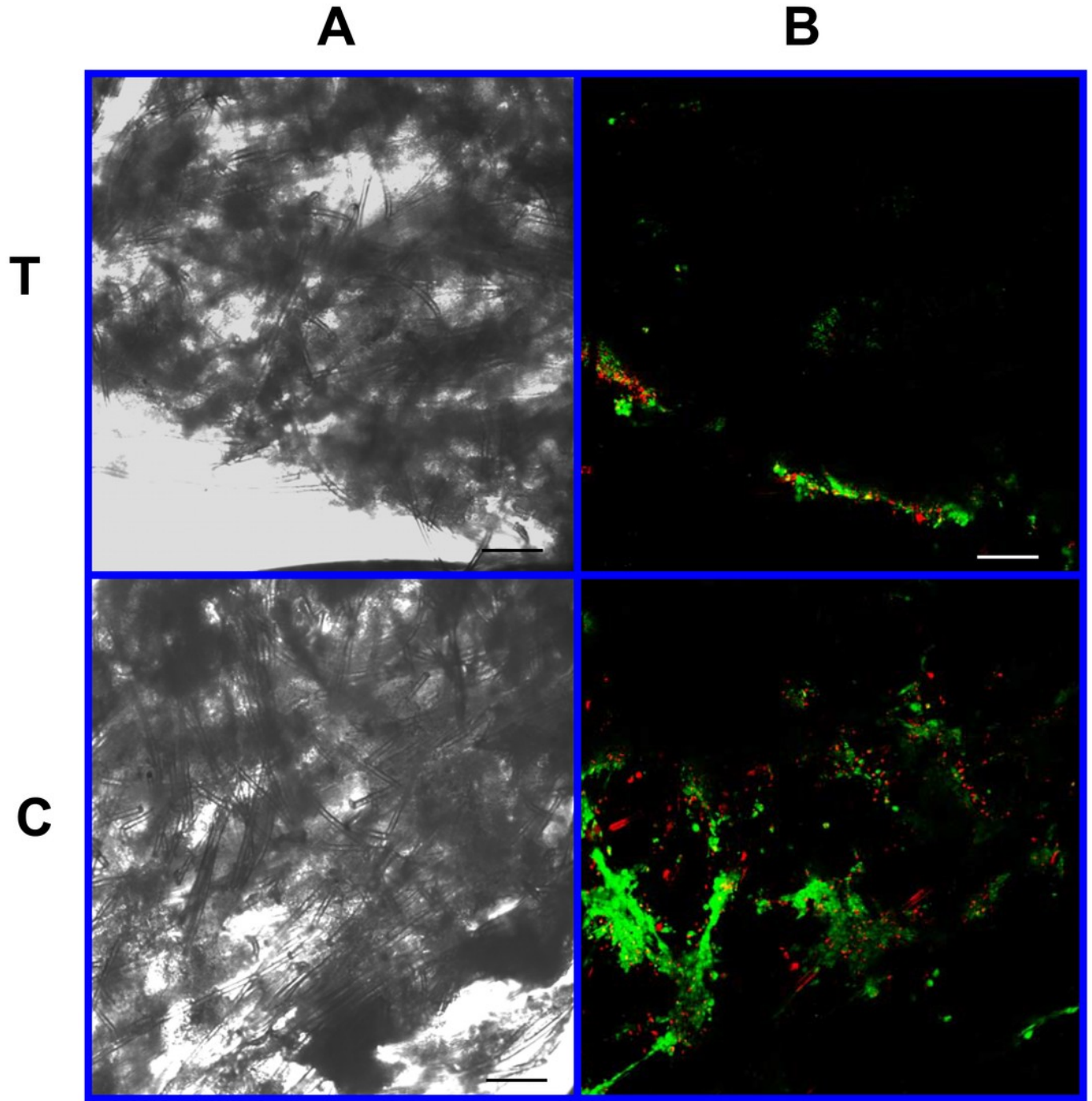


Figure 9

Synoviocytes cultured on 2% PLLA coated PGA on day 21 of dynamic culture.

Photomicrographs of 2% PLLA coated PGA constructs harvested on day 21, under standard light (column **A**) and under laser confocal microscopy (column **B**), using the calcein AM-ethidium homodimer live-dead assay. Images represent scaffold transverse cross sections (row **T**) and scaffold surface coronal sections (row **C**). Green stained cells are alive, red stained cells are dead. Note the spurious red staining of scaffold PGA fibers. 10x objective magnification; bar = 100 μ m

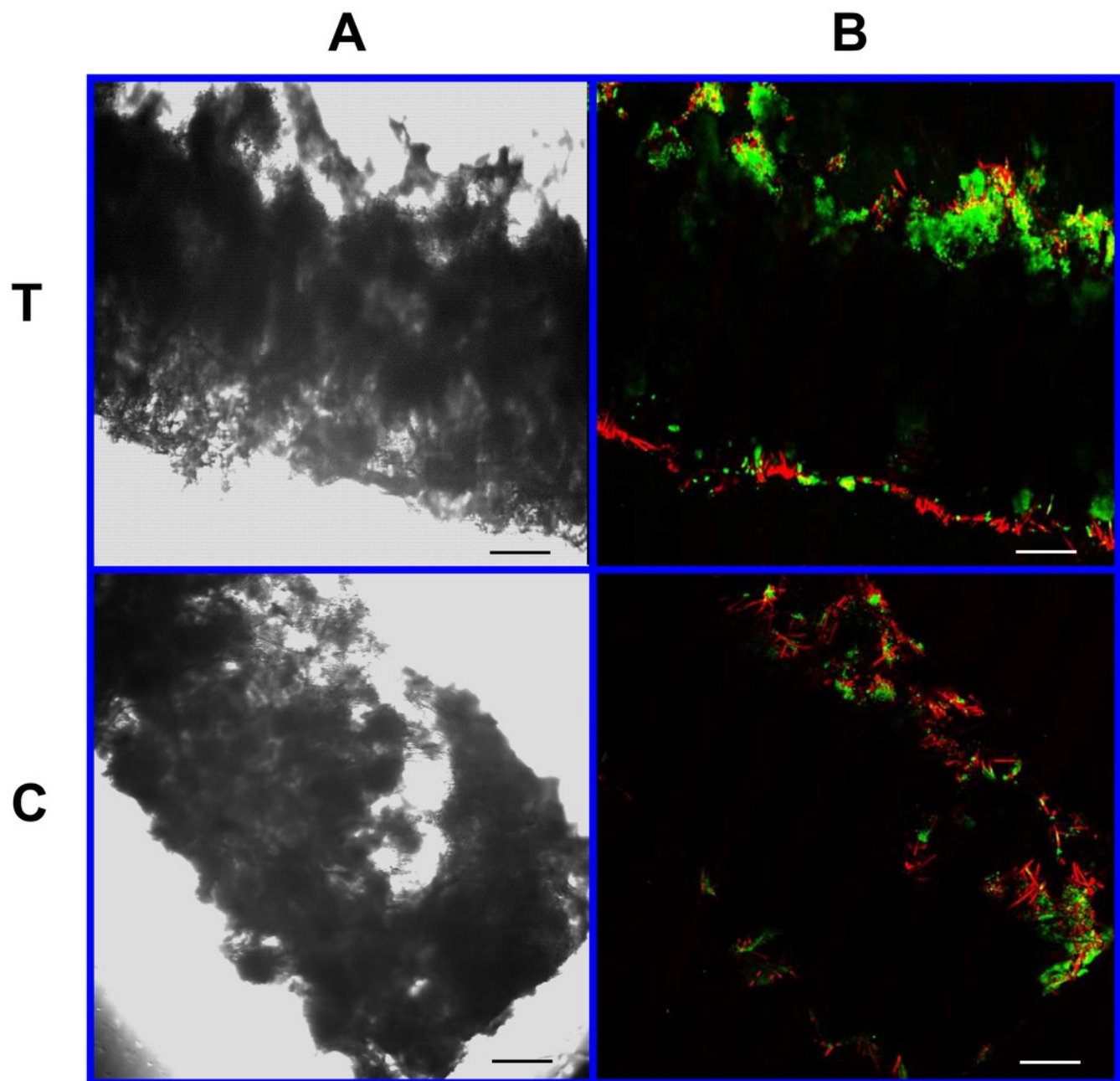


Figure 10

Synoviocytes cultured on 4% PLLA coated PGA on day 10 of dynamic culture.

Photomicrographs of 4% PLLA coated PGA constructs harvested on day 10, under standard light (column **A**) and under laser confocal microscopy (column **B**), using the calcein AM-ethidium homodimer live-dead assay. Images represent scaffold transverse cross sections (row **T**) and scaffold surface coronal sections (row **C**). Green stained cells are alive, red stained cells are dead. Note the spurious red staining of PGA fibers. 10x objective magnification; bar = 100µm.

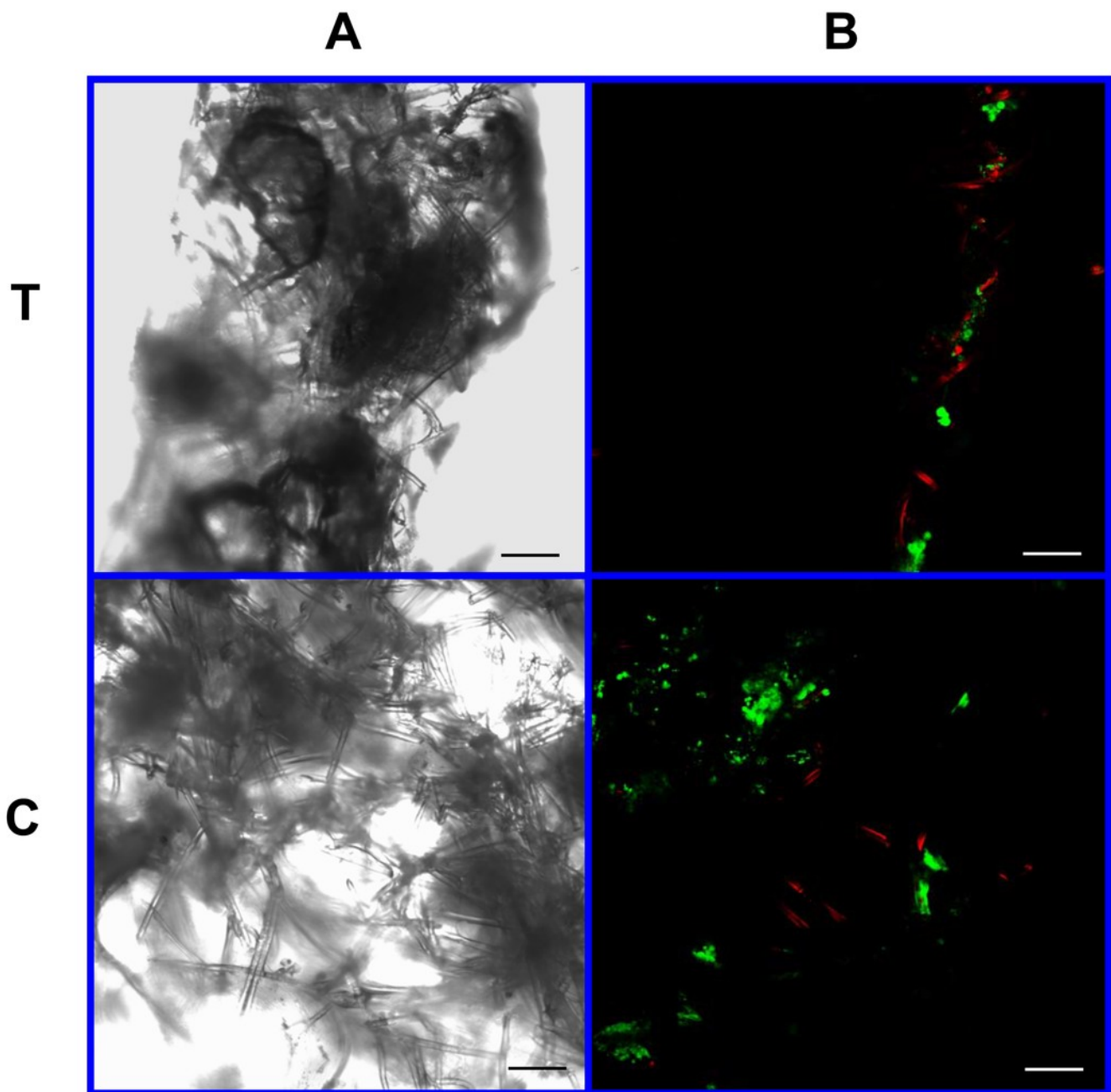


Figure 11

Synoviocytes cultured on 4% PLLA coated PGA on day 21 of dynamic culture .

Photomicrographs of 4% PLLA coated PGA constructs harvested on day 21, under standard light (column **A**) and under laser confocal microscopy (column **B**), using the calcein AM-ethidium homodimer live-dead assay. Images represent scaffold transverse cross sections (row **T**) and scaffold surface coronal sections (row **C**). Green stained cells are alive, red stained cells are dead. Note the spurious red staining of PGA fibers. 10x objective magnification; bar = 100 μ m.

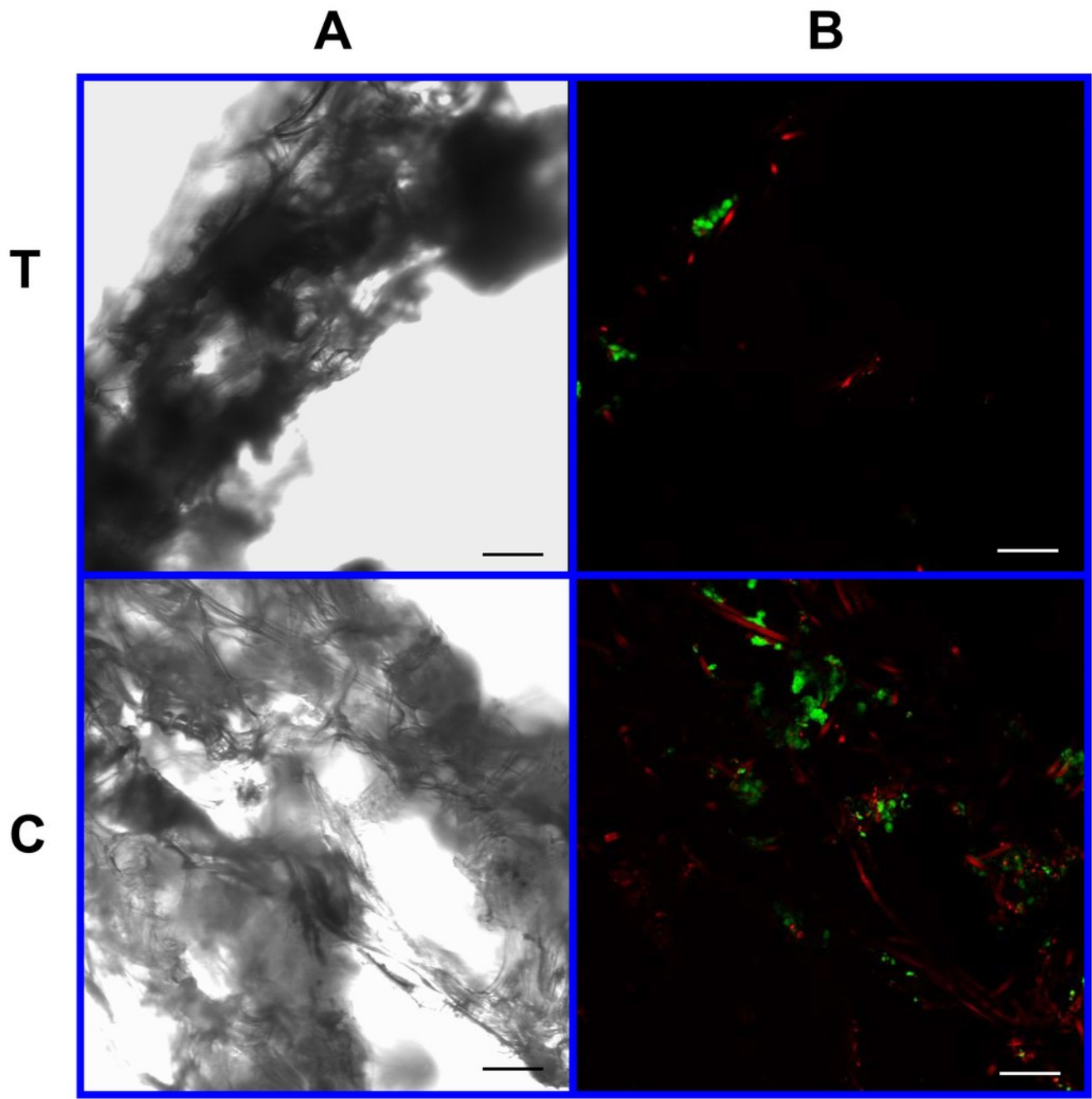


Figure 12

Cellular distribution on PLLA coated PGA scaffolds.

Photomicrographs of 2% PLLA coated PGA scaffolds harvested on day 10 (row 1) and day 21 (row 2), and 4% PLLA coated PGA scaffolds harvested on day 10 (row 3) and day 21 (row 4), H+E staining. Column A represents images of the center of the construct and column B represents images taken of the scaffold periphery. Note that the cells have grown in dense clusters; 10x objective magnification; bar = 100 μ m.

